Modeling of Lattice Parameter in the Ni-Al System

TAO WANG, JINGZHI ZHU, REBECCA A. MACKAY, LONG-QING CHEN, and ZI-KUI LIU

Considering the effects of temperature and composition, a phenomenological description of lattice parameters in solid states was developed. The lattice parameter of the pure element is modeled under the assumption of a linear temperature dependence of thermal expansion, while the lattice parameters of substitutional solid-solution phases are treated similar to the Gibbs-energy modeling in the CALPHAD (CALculation of PHAse Diagram) approach. Using this model, the lattice parameters of the γ and γ' phases in the Ni-Al system were analyzed and the model parameters were evaluated. The calculated lattice parameters and mismatches show good agreement with existing experimental data.

I. INTRODUCTION

THE lattice parameter and thermal expansion are two important material properties that are strongly correlated to many thermophysical properties. Because of their importance in both theoretical study and practical applications, a large number of studies have been done on this subject from many different points of view, using theoretical, experimental, and empirical approaches.

The composition dependency of lattice parameters was modeled in various ways, such as elasticity theory, various potential approaches, and first-principle calculation, but none of them is very successful:[1] they are neither simple nor accurate enough. The most frequently used prediction of the lattice parameters across a solid solution was the linear relationship proposed by Vegard.[2] However, the investigations on metallic systems always show some deviations from Vegard's law, because Vergard's law is only valid when the electronic environment of both kinds of atoms is undisturbed by the formation of the solid solution, but, in reality, electrons in states just below the Fermi level can also participate in metallic bonding.[3]

Due to the limited and scattered experimental data, the temperature effect on the lattice parameter is often overlooked, especially for multicomponent alloys. In many cases, such an effect is assumed to be small enough to be neglected or approximated by some arbitrary polynomials (the linear relationship is often suggested). However, such an assumption is seldom supported by the experimental results, except in a very narrow temperature region.

In the present work, a simple phenomenological model is developed to describe the lattice parameters of solid-solution phases as a function of their composition and temperature. The temperature effect on the linear-expansion coefficient (α_L) of the pure element is considered first, and then the lattice parameters of pure elements are then calculated from the thermal expansion. The contribution from substitutional solute is treated using an approach similar to that used in the Gibbs-energy modeling.[4] At the end of the Section II, the modeling of the chemical-ordering effect will be discussed in relation to the sublattice model.

Nickel-based superalloys are used for the manufacture of aircraft turbine blades because of their good mechanical properties at high temperatures. Many investigations indicated that the difference between the lattice parameters of precipitate γ' ($L1_2$) and matrix γ (fcc_A1) plays a very important role in the microstructure evolution and properties of Ni-based superalloys.[5–8] In Section III, we apply our model to the Ni-Al system, the most important constituent binary system in Ni-based superalloys. We evaluate the model parameters of the γ' and γ phases to describe their lattice parameters and calculate the lattice difference between the γ' and γ phases.

II. MODELS

A. *Pure Element*

Based on quantum physics, Ruffa[9] proposed the following equation to describe the thermal-expansion coefficients:

$$\alpha_L = \frac{3k}{2wr_nD}\left(\frac{T}{\theta_D}\right)^3 g(x_D) \qquad [1]$$

where T is the temperature; k is Boltzmann's constant; w and D are the inverse width and depth, respectively, of the Morse potential; r_n is the nearest-neighbor distance; θ_D is the Debye temperature, and $x_D = \theta_D/T$. The integral $g(x_D)$ is given by

$$g(x_D) = \int_0^{x_D} \frac{x^4 e^x}{(e^x - 1)^2}\, dx \qquad [2]$$

Since Eq. [1] only considers the first order in the frequency, it is usually accurate only up to about $0.7\theta_D$, but gives the dominant contribution over the entire temperature range. To extend this formula to higher temperatures, a correction term was added:[9]

$$\alpha_L = \frac{3k}{2wr_nD}\left(\frac{T}{\theta_D}\right)^3 \left(g(x_D) + \frac{kT}{2D} g_1(x_D)\right) \qquad [3]$$

where

$$g_1(x_D) = \int_0^{x_D} \frac{x^5 e^x (1 + e^x)}{(e^x - 1)^3}\, dx \qquad [4]$$

TAO WANG, Ph.D. Student, JINGZHI ZHU, Postdoctoral Scholar, LONG-QING CHEN, Professor, and ZI-KUI LIU, Associate Professor, are with the Department of Materials Science and Engineering, The Pennsylvania State University, University Park, PA 16802. Contact e-mail: taowang@psu.edu REBECCA A. MACKAY, Senior Materials Scientist, is with the Materials Division, NASA Glenn Research Center, Cleveland, OH 44135.

Manuscript submitted June 30, 2003.

For low temperatures ($T \ll \theta_D$), one can obtain

$$\alpha_L \approx \frac{2k\pi^4}{5wr_nD}\left(\frac{T}{\theta_D}\right)^3 \quad [5]$$

which implies that α_L is proportional to T^3 for $T \ll \theta_D$.

When the temperature is high ($T \gg \theta_D$),

$$\alpha_L \approx \frac{3k}{2wr_nD}\left(\left(\frac{1}{3}+\frac{3k\theta_D}{8D}\right)+\frac{k}{3D}T+\left(\frac{\theta_D}{4}+\frac{k\theta_D^2}{10D}\right)\frac{1}{T}\right) \quad [6]$$

Because the contribution of the $1/T$ term is not significant at high temperatures, α_L varies almost linearly with temperature in the high-temperature range, which will be adopted in the present work, *i.e.,* we can describe the thermal-expansion coefficient by a linear function of temperature as a first approximation.

$$\alpha_L = A + BT \quad [7]$$

The parameters A and B can be defined by available information from the thermal-expansion experiments. Such a linear relationship was observed by several investigations.[10,11,12]

The lattice parameter (a) can be obtained from Eq. [7] through integration of α_L based on the definition $\alpha_L = 1/a \times da/dT$, and the lattice parameter (a_0) at a given temperature (T_0) can be used to determine the integration constant:

$$a = a_0 \exp\left(A(T - T_0) + \frac{B}{2}(T^2 - T_0^2)\right) \quad [8]$$

The value of α_L is about $10^{-5}\ K^{-1}$ for metals, so the relative change in lattice parameter is very small (about 1 pct with a change of 1000 K in temperature); thus, the lattice parameter can be approximated by the following polynomial:

$$a = a_0\left(A(T - T_0) + \frac{B}{2}(T^2 - T_0^2) + 1\right) \quad [9]$$

In Section III, we calculate the lattice parameters of Al by both Eqs. [8] and [9], and the results are almost identical.

B. *Binary System*

Similar to the Gibbs-energy modeling,[4] we add an excess contribution to describe the deviation of the lattice parameter from the Vegard's law. Such a phenomenological model can be written as

$$a = \sum_i x_i {}^0a_i + {}^{ex}a \quad [10]$$

where x_i is the mole fraction of element i; ${}^0a_i$ denotes the lattice parameter of pure element i defined by Eq. [9]; and ${}^{ex}a$ is the excess contribution expressed in the Redlich–Kister polynomials:[13]

$${}^{ex}a = \sum_i \sum_{j>i} x_i x_j \sum_{k=0}^{n} {}^kI_{i,j}(x_i - x_j)^k \quad [11]$$

The interaction parameter (${}^kI_{i,j}$) can be expressed as a function of temperature:

$${}^kI_{i,j} = {}^kA_{i,j} + {}^kB_{i,j}T \quad [12]$$

C. *Ordered Phase*

The ordered phase and related disordered phase can be modeled by the sublattice model.[14,15] For a two-sublattice model, $(A, B)_p\ (A, B)_q$, the lattice parameter a can be expressed by the following equation:

$$a = \sum_i \sum_j y_i^{\mathrm{I}} y_j^{\mathrm{II}} {}^0a_{i:j} + \sum_i \sum_{j>i} y_i^{\mathrm{I}} y_j^{\mathrm{I}} \sum_k y_k^{\mathrm{II}} \mathrm{I}_{i,j:k} + \sum_i \sum_{j>i} y_i^{\mathrm{II}} y_j^{\mathrm{II}} \sum_k y_k^{\mathrm{I}} \mathrm{I}_{k:i,j} + \sum_i \sum_{j>i} \sum_k \sum_{l>k} y_i^{\mathrm{I}} y_j^{\mathrm{I}} y_k^{\mathrm{II}} y_l^{\mathrm{II}} \mathrm{I}_{i,j:k,l} \quad [13]$$

where y_i^{I} and y_i^{II} are the site fractions of i in the first and second sublattices. Similar to Eq. [12], the interaction parameters $I_{i,j:k}$, $I_{k:i,j}$, and $I_{i,j:k,l}$ can be expressed as functions of temperature. The term ${}^0a_{i:j}$, the lattice parameter of the end member $i_p j_q$ of the sublattice model, can be written as

$${}^0a_{i:j} = \begin{cases} {}^0a_i & j = i \\ \dfrac{p}{p+q}{}^0a_i + \dfrac{q}{p+q}{}^0a_j + C_{i:j} + D_{i:j}T & j \neq i \end{cases} \quad [14]$$

where $C_{i:j}$ and $D_{i:j}$ are model parameters.

The overall composition (x_i) is connected with the site fractions by $x_i = p(p+q) \times y_i^{\mathrm{I}} + q(p+q) \times y_i^{\mathrm{II}}$. When $x_i = y_i^{\mathrm{I}} = y_i^{\mathrm{II}}$, the phase is disordered, and Eq. [13] is equivalent to Eq. [10].

III. APPLICATION TO Ni-Al SYSTEM

In this section we will apply the previous phenomenological model to describe the lattice parameters of γ' and γ phases in the Ni-Al system.

A. *Pure Al and Ni*

Many reports on the measurement of thermal-expansion coefficients and lattice parameters for Al can be found in the literature. Touloukian *et al.*[16] referenced 71 sets of data for Al in their review, and later, Wang and Reeber[17] cited seven more in their report. Their selection of experimental data are shown in Figure 1. Because the model is not applicable to the low-temperature range, only the experimental data measured above 300 K are used to evaluate the parameters A and B in Eq. [7]. The results are plotted as the solid line in Figure 1.

As shown in Figure 1, the coefficient of linear thermal expansion for Al shows a good linear relationship with temperature from 300 to 800 K (standard deviation of $S_N = 7 \times 10^{-7}\ K^{-1}$, calculated as the square root of the sample variance of a set of values[18]). The low-temperature behavior deviates from the linearity because the model only accurately describes the intermediate-temperature behavior. When the temperature is very high (close to the melting temperature T_m), the experimental results show a visible deviation from the linear dependence, which is caused by the contribution from thermal vacancies.[17]

Based on the model parameters obtained from the previous evaluation, the lattice parameter of Al can be calculated by Eq. [8] or [9]. Figure 2 shows the calculated lattice parameters compared with the experimental data, and it can be seen that most experimental data can be well reproduced

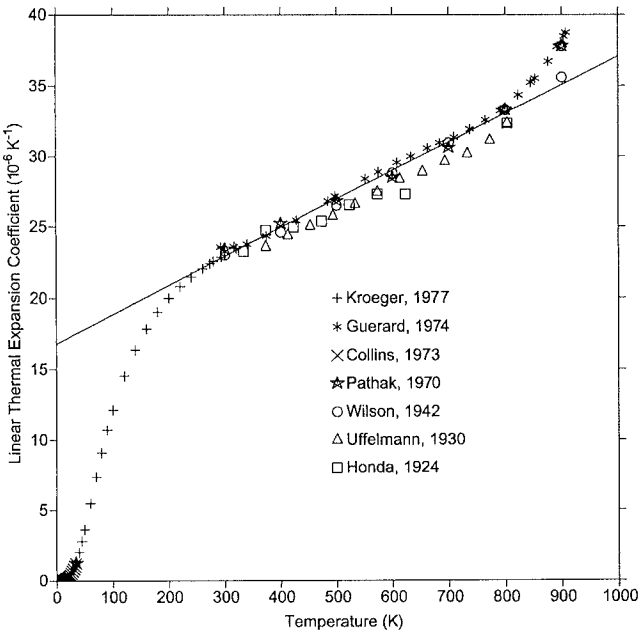

Fig. 1—Calculated linear thermal expansion coefficient of fcc Al (solid line $\alpha = 1.68 \times 10^{-5} + 2.03 \times 10^{-8} T$ and $S_N = 1.1 \times 10^{-6}$ K^{-1} for $T > 300$ K) in comparison with experimental data from the literature (△, [10] ☆, [12] +, [66] ∗, [67] ×, [68] ○, [69] and □ [70]).

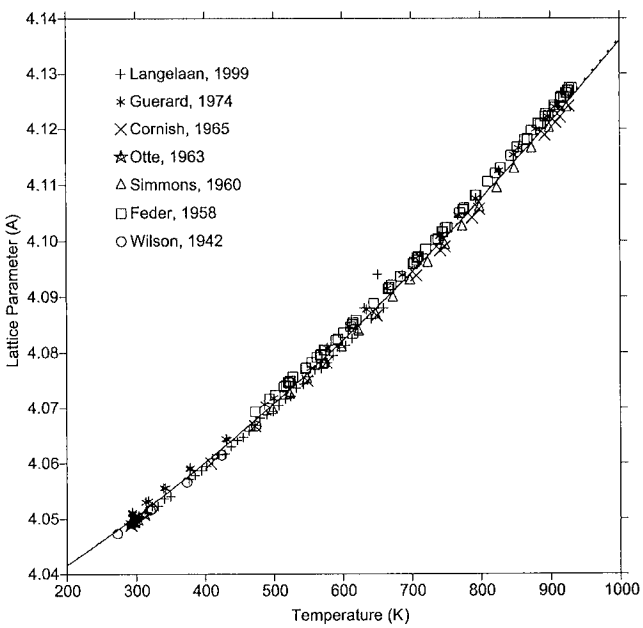

Fig. 2—Comparison of lattice parameter data for Al and the model calculation (∗, [67] ○, [69] +, [71] ×, [72] ☆, [73] △, [74] and □ [75]). The dotted and solid lines represent the results from Eq. [8] ($a = 4.0708 \exp[1.68 \times 10^{-5} (T - 500) + 1.01 \times 10^{-8} (T^2 - 500^2)]$ and $S_N = 1.3 \times 10^{-3}$ Å) and Eq. [9] ($a = 4.0708 \times [1.68 \times 10^{-5} (T - 500) + 1.01 \times 10^{-8} (T^2 - 500^2) + 1]$ and $S_N = 1.3 \times 10^{-3}$ Å).

by the present model ($S_N = 1.3 \times 10^{-3}$ Å). As shown in Figure 2, when the temperature increases from room temperature to the melting temperature, the lattice parameter of Al only increases 2 pct. The dotted and solid lines represent the results from Eqs. [8] and [9], respectively, and the differences between them are less than 0.015 pct.

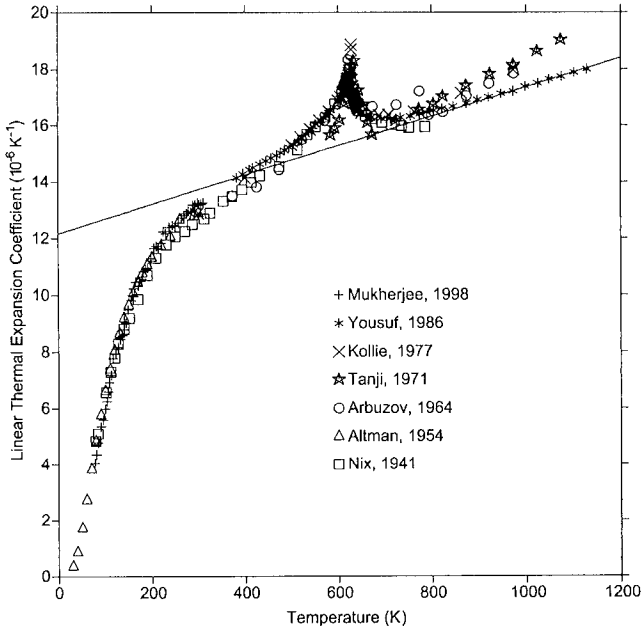

Fig. 3—Calculated linear thermal expansion coefficient of fcc Ni (solid line $\alpha = 1.22 \times 10^{-5} + 0.52 \times 10^{-8} T$ and $S_N = 1.3 \times 10^{-6}$ K^{-1} for $T > 300$ K) in comparison with experimental data from the literature (×, [19] +, [20] ∗, [21] ☆, [22] ○, [23] △, [24] and □ [25]).

Many experimental studies on the thermal expansion of Ni were performed in a wide temperature range, and more than 100 investigations before 1975 have been reviewed by Touloukian *et al.*[16] Using the dilatometry technique, Kollie[19] measured thermal expansions in the temperature range from 300 to 1000 K, while Mukherjee *et al.*[20] investigated thermal expansions for low temperatures up to 300 K. Yousuf *et al.*[21] studied the magnetic effect on the lattice expansion of Ni by high-temperature X-ray diffractometry and reported the lattice parameters and the thermal-expansion coefficients. The data[19–25] are plotted in Figure 3. The experimental data show a clear peak around the Curie temperature T_C (633 K) of Ni, which means that the magnetic phase transition has a significant effect on the thermal expansion. In the low-temperature range, the experimental results are in good agreement with each other. However, at the high temperatures, the thermal-expansion coefficient by Yousuf *et al.* is lower than those in previous reports.[22,23] Since the purity of their samples[21] is higher than the others, the results from Yousuf *et al.* were used to determine the model parameters in Eq. [7] in the present work. The calculated linear thermal-expansion coefficient of Ni is shown in Figure 3 as the solid line. The low-temperature data ($T < 300$ K) were not used in the parameter determination and deviate from the solid line because Eq. [7], as discussed in the previous section, is only applicable in the high-temperature range.

Lattice parameters for Ni have been measured by many investigators.[21,26–29] But, the agreements among their results are quite poor, especially in the high-temperature range. One of the possible reasons is the effect of magnetism, which was recently emphasized by many investigators.[20,21,30] Figure 4 plots the selected data from the literature. The poor agreements between the experimental data from different researchers can be observed in the high-temperature range. It, therefore, seems difficult to define a suitable mathematic

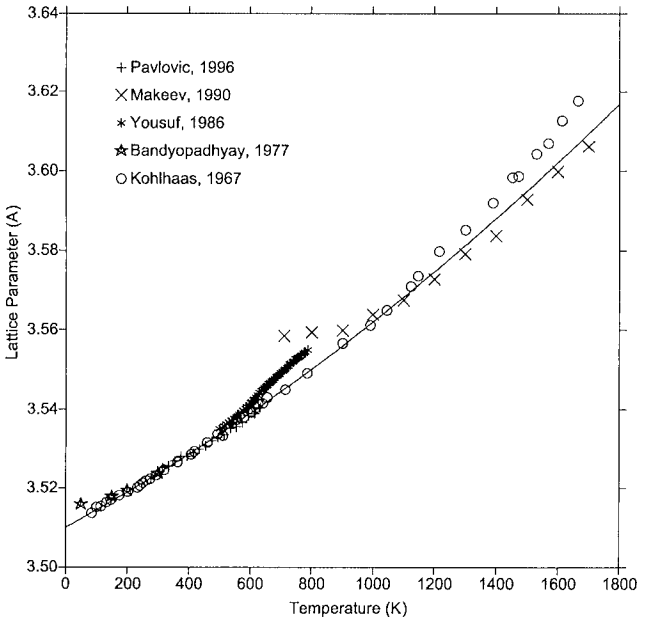

Fig. 4—Comparison of lattice parameter data for Ni (✳, [21] +, [26] ×, [27] ☆, [28] and ○ [29]) and the model calculation (solid line $a = 3.5560 \times [1.22 \times 10^{-5} (T - 900) + 0.26 \times 10^{-8} (T^2 - 900^2) + 1]$ and $S_N = 3.6 \times 10^{-3}$ Å).

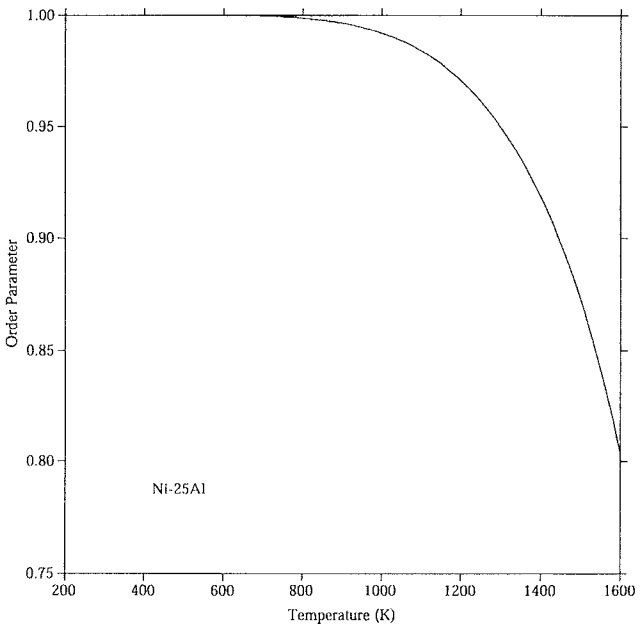

Fig. 5—Order parameter *vs* temperature curve for the Ni-25 at. pct Al alloy.

description just on the basis of the experimental lattice-parameter data.

After determining the model parameters in Eq. [7] from the previous experimental thermal-expansion data, the lattice parameter of Ni can be calculated from Eq. [9]. The calculated lattice parameter is shown in Figure 4 by the solid line. In the low-temperature range ($T < T_c$), the experimental values are well reproduced by the calculation $S_N = 1.5 \times 10^{-3}$ Å. At high temperatures, although the available experimental data are relatively scattered, our modeling still shows a reasonable description ($S_N = 5.1 \times 10^{-3}$ Å). As shown in Figures 3 and 4, changes of slopes of both the thermal expansion and lattice parameter near the Curie temperature were observed experimentally. To reproduce the phenomena requires a more accurate model that takes into account the magnetic effect.

In the present work, we chose a T_0 value in Eqs. [8] and [9] of $T_m/2$, and a_0 was evaluated from the available experimental data of the lattice parameter.

B. *Binary Ni-Al System*

1. *Experimental data*

The lattice parameters of the γ solid solution in the Ni-Al system were measured by several groups.[31–37] Most of those values were measured at room temperature on samples quenched from high temperatures. The temperature dependence of the lattice parameter of Ni-Al alloys was investigated by Kamara *et al.*[32] using high-temperature X-ray diffractometry. Another *in-situ* X-ray measurement was performed by Bottiger *et al.*[31] on five different alloy compositions, and the lattice parameters up to 553 K were reported.

The room-temperature lattice parameters of the γ' phase were determined by many investigators[32,33,36–51] on samples quenched mostly from 1173 to 1473 K. The temperature effect on the γ' phase was studied by Arbazov and Zelenkov in the temperature range of 293 to 974 K[23] and by Taylor and Floyd for 74 to 1273 K[36] using the dilatometry technique, and their results on the relative thermal expansion agree with each other. Using high-temperature X-ray diffractometry, Kamara *et al.*,[32] Rao *et al.*,[52] and Stoeckinger and Neumann[45] investigated the temperature dependencies of the γ' lattice parameter. A typical experimental method includes four steps: sample preparation, heat treatment (homogenization or aging), quenching, and measurement (mostly at room temperature). Kamara's experiment procedure[32] can be described briefly as follows:

1. prepared the Ni-17.7 at. pct Al alloy by arc melting,
2. homogenized the samples at 1273 K for 30 minutes and age them at 973 K for 168 hours,
3. quenched the annealed sample to room temperature, and
4. measured the lattice parameters at different temperatures (293, 563, 713, 843, and 953 K) for 0.6 to 2 hours.

The measured lattice-parameter value is strongly affected by experimental details. On one hand, the measuring temperature has a direct effect on the lattice parameter because of the thermal expansion; on the other hand, many experimental conditions can also impact the lattice parameter by changing the composition and the order parameters of phases.

The order parameter η, the degree of ordering, can be calculated by the site fraction of various elements in the ordered phase. For γ' in the Ni-Al system, the order parameter can be defined as

$$\eta = \frac{y_{Al}^{II} - y_{Al}^{I}}{3y_{Al}^{I} + y_{Al}^{II}} \quad [15]$$

where y_{Al}^{I} and y_{Al}^{II} are the site fractions of Al in the first and second sublattices, respectively.

Using the thermodynamic descriptions by Dupin *et al.*,[53,54] the change of the order parameter with temperature is shown in Figure 5 for the Ni-25 at. pct Al alloy. Obviously, the

order parameter changes very little in the low-temperature range.

During measurement, the compositions of phases change with the measurement temperature and the measurement time. This evolution can be simulated by the Dictra software.[55] The thermodynamic database from Dupin and co-workers[53,54] and the mobility database from Engstrom and Agren[56] were used in the simulation. Since the diffusivity in the γ' ordered phase is much smaller than that in the γ disordered phase (about one order of magnitude smaller in the Ni-Al system[57]), only the diffusion in the γ phase was considered in the present simulation. The average simulation size of the γ phase ($\sim$1.5 μm) and the measurement temperatures (293, 563, 713, 843, and 953 K) were obtained from Kamara's experiment,[32] and the initial composition (12.18 at. pct Al) is taken as the equilibrium compositions at the aging temperature (973 K). The change of the average composition in the γ phase at 953 K (the highest measurement temperature in Kamara's experiment[32]) is shown in Figure 6, and the two dashed lines refer to the initial composition and the equilibrium composition at 953 K, respectively. According to this figure, the composition will not change significantly during the measurement (usually less than 3 hours) if the temperature is lower than 953 K.

We can, thus, assume that the compositions of the samples measured below the aging temperature are the same as those at the aging temperature (frozen-composition assumption).

2. *Evaluation of model parameters*

According to Eq. [10], the lattice parameters of the γ disordered solution can be described as

$$a = x_{Al}{}^0a_{Al} + x_{Ni}{}^0a_{Ni} + x_{Al}x_{Ni}(A_{Al,Ni} + B_{Al,Ni}T) \quad [16]$$

The terms $A_{Al,Ni}$ and $B_{Al,Ni}$ are model parameters to be evaluated from the experimental data of the γ phase.

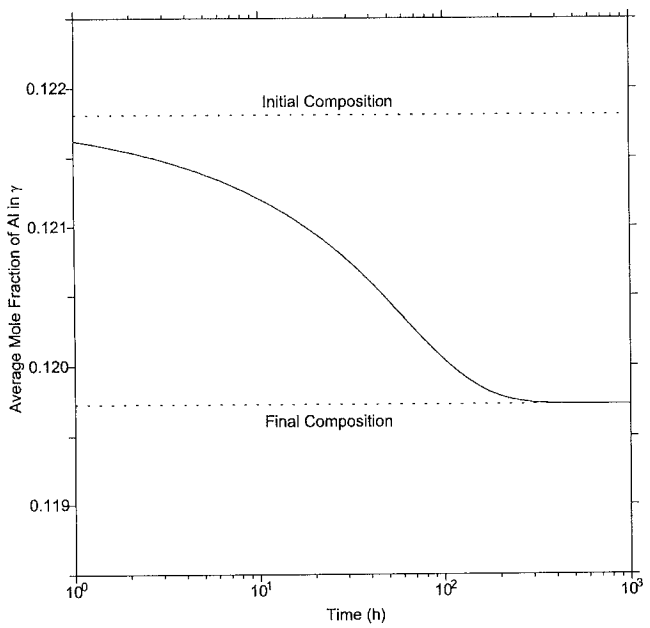

Fig. 6—Average composition in the γ phase as a function of the holding time during measurement at 953 K. The initial and final compositions (dotted lines) refer to the equilibrium compositions at the previous annealing temperature (973 K) and the measurement temperature (953 K), respectively.

As the γ and γ' phases are described with one single Gibbs energy by two sublattices using the formula $(Al,Ni)_3(Al,Ni)_1$,[54] for the γ' phase, Eq. [14] is rewritten as

$$^0a_{Al:Al} = {}^0a_{Al} \quad [17]$$

$$^0a_{Ni:Ni} = {}^0a_{Ni} \quad [18]$$

$$^0a_{Ni:Al} = 0.25{}^0a_{Al} + 0.75{}^0a_{Ni} + C_{Ni:Al} + D_{Ni:Al}T \quad [19]$$

$$^0a_{Al:Ni} = 0.75{}^0a_{Al} + 0.25{}^0a_{Ni} + C_{Al:Ni} + D_{Al:Ni}T \quad [20]$$

Due to the limited experimental data, the following assumptions were made to reduce the number of independent parameters:

$$I_{Ni,Al:Al,Ni} = 0 \quad [21]$$

$$I_{*:Al,Ni} = A_{*:Al,Ni} + B_{*:Al,Ni}T \quad [22]$$

$$I_{Ni,Al:*} = 3I_{*:Al,Ni} = 3(A_{*:Al,Ni} + B_{*:Al,Ni}T) \quad [23]$$

where the asterisk refers to Al or Ni. Thus, Eq. [13] can be simplified to

$$a = y^I_{Al}y^{II}_{Al}{}^0a_{Al:Al} + y^I_{Al}y^{II}_{Ni}{}^0a_{Al:Ni} + y^I_{Ni}y^{II}_{Al}{}^0a_{Ni:Al} + y^I_{Ni}y^{II}_{Ni}{}^0a_{Ni:Ni} + 3y^I_{Al}y^I_{Ni}I_{*:Ni,Al} + y^{II}_{Al}y^{II}_{Ni}I_{*:Al,Ni} \quad [24]$$

Since $x_i = 0.75y'_i + 0.25\,y''_i$, and the phase is disordered when $x_i = y'_i = y''_i$, we obtain

$$\begin{cases} 4A_{*:Al,Ni} + C_{Ni:Al} + C_{Al:Ni} = A_{Al,Ni} \\ 4B_{*:Al,Ni} + D_{Ni:Al} + D_{Al:Ni} = B_{Al:Ni} \end{cases} \quad [25]$$

Using the experimental lattice-parameter values of the γ' phase and the previously obtained parameters $A_{Al,Ni}$ and $B_{Al,Ni}$, the parameters of the ordered phase were evaluated by the parrot module of the Thermo-Calc software.[55] The compositions and the site fractions used in the present work were calculated from the thermodynamic descriptions by Dupin *et al.*[53,54] All available experimental data were selected in the present evaluation of model parameters, and the data obtained at room temperature were given very low weight because of the large discrepancies.

3. *Results and discussion*

All model parameters for the lattice parameters of the γ and γ' phases in the Ni-Al system are listed in Table I. It is shown that the lattice parameter of Al has a higher temperature dependence than that of Ni. The Ni_3Al has a rather weak temperature-dependent lattice parameter, while the hypothetic Al_3Ni phase has the highest temperature dependence. The interaction parameter is negative and becomes more negative with increasing temperature, which reduces the lattice mismatch between γ and γ', as discussed later.

Table I. The Optimized Parameters for the γ and γ' Phases in Ni-Al System (in Å)

$^0a_{Al:Al} = 4.0262 + 6.8572 \times 10^{-5}\,T + 4.1237 \times 10^{-8}T^2$
$^0a_{Ni:Ni} = 3.5098 + 4.3266 \times 10^{-5}\,T + 9.2456 \times 10^{-9}\,T^2$
$^0a_{Ni:Al} = 0.75{}^0a_{Ni:Ni} + 0.25{}^0a_{Al:Al} - 8.5743 \times 10^{-2} - 8.4818 \times 10^{-6}\,T$
$^0a_{Al:Ni} = 0.25{}^0a_{Ni:Ni} + 0.75{}^0a_{Al:Al} - 1.1893 \times 10^{-1} + 1.7764 \times 10^{-4}\,T$
$I_{Al,Ni:*} = -1.4516 \times 10^{-1} - 1.2687 \times 10^{-4}\,T$
$I_{*:Al,Ni} = -4.8385 \times 10^{-2} - 4.2290 \times 10^{-5}\,T$

The composition dependence of the lattice parameter of the γ solid solution at room temperature is calculated and compared with experimental data in Figure 7, and the calculated lattice parameters as a function of temperature for various compositions are plotted with experimental values in Figure 8. Although the trends with temperature are similar, results by Bottiger *et al.*[31] are significantly smaller than those reported by Kamara *et al.*[32] It is, therefore, impossible to reproduce both sets of data. The same situation appears in the room-temperature data in Figure 7, where the values reported by Bottiger *et al.* are smaller than other available data.[33–35,58] Since Bottiger's investigation was performed on thin-film samples from sputtering, their results are likely to be influenced by several processing factors. For example, Bottiger *et al.* found that a higher sputtering pressure will reduce the lattice parameter. All experimental data except for those from Bottiger *et al.* were selected for the evaluation of model parameters, and the calculation can represent most of those experimental data reasonably well ($S_N = 4.1 \times 10^{-3}$ Å).

The lattice parameters of the γ' phase measured at room temperature are plotted in Figure 9, and they are quite scattered. Compared with measurements of the disordered phase, the lattice parameter of the ordered phase is much more sensitive to experimental procedures, *e.g.*, heat-treatment temperature and time. The treatment history will change the composition and order parameter and then cause large discrepancies in the measured lattice parameters. The composition dependence of the lattice parameter of the γ' phase at room temperature was calculated by the present model as the solid line in Figure 9, and the standard deviation is 7.4×10^{-3} Å. The calculated curve lies among the experimental data and displays a similar slope to those reported by Noguchi *et al.*[43] and Aoki and Izumi.[44]

The calculated temperature dependence of the γ'-phase lattice parameter is compared with the experimental data in Figure 10. Both the data by Kamara *et al.*[32] and Stoeckinger and Neumann[45] can be well reproduced by our model (Figures 10(a) and (b), $S_N = 2.5 \times 10^{-3}$ and 2.7×10^{-3},

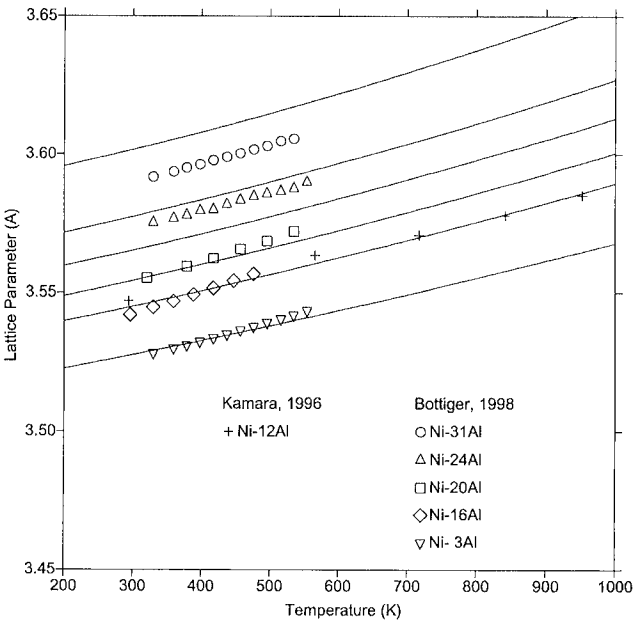

Fig. 8—Temperature dependence of the lattice parameter of the γ phase in various Ni-Al alloys (○, △, □, ◇, ▽, [31] and + [32]). The solid lines represent the results of the model calculation ($S_N = 7.9 \times 10^{-3}$ Å for Ref. 31 and $S_N = 1.7 \times 10^{-3}$ Å for Ref. 32).

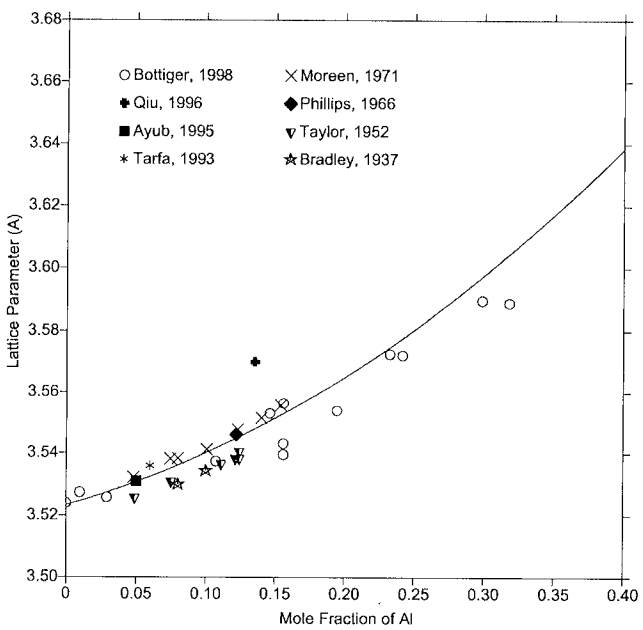

Fig. 7—Room-temperature lattice parameter of the γ phase in the Ni-Al system (○, [31], ✚, [33] ■, [34] ∗, [35], ▼ [36] ◆, [48], ☆ [51] and × [58]). The solid line represents the results of the the model calculation ($S_N = 6.4 \times 10^{-3}$ Å).

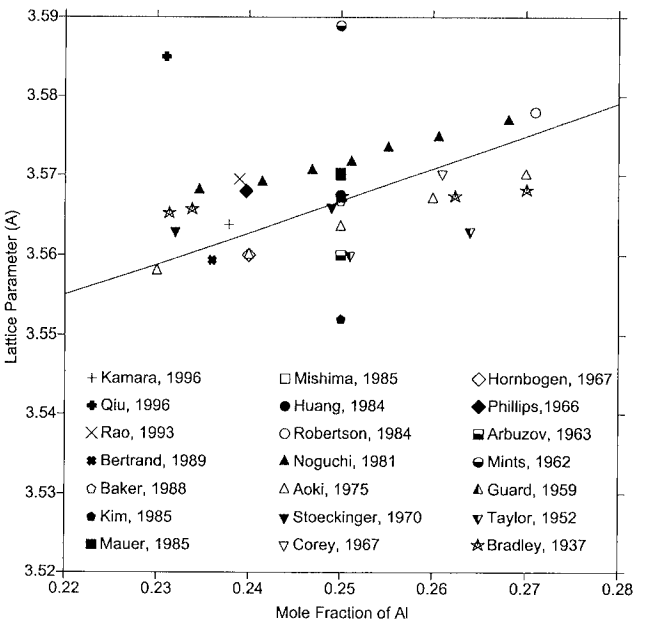

Fig. 9—Room-temperature lattice parameter of the γ' phase (+, [32] ✚, [33] ▼, [36] □, [37] ×, [38] ✖, [39] ⬡, [40] , ⬟ [41] ●, [42] ▲, [43] △, [44] ▼, [45] ▽, [46] ◇, [47] ◆, [48] , ⬓ [49] ◭, [50] ☆, [51] ■, [76] ○, [77] and ◒ [78]). The solid line represents the results of the model calculation ($S_N = 7.4 \times 10^{-3}$ Å).

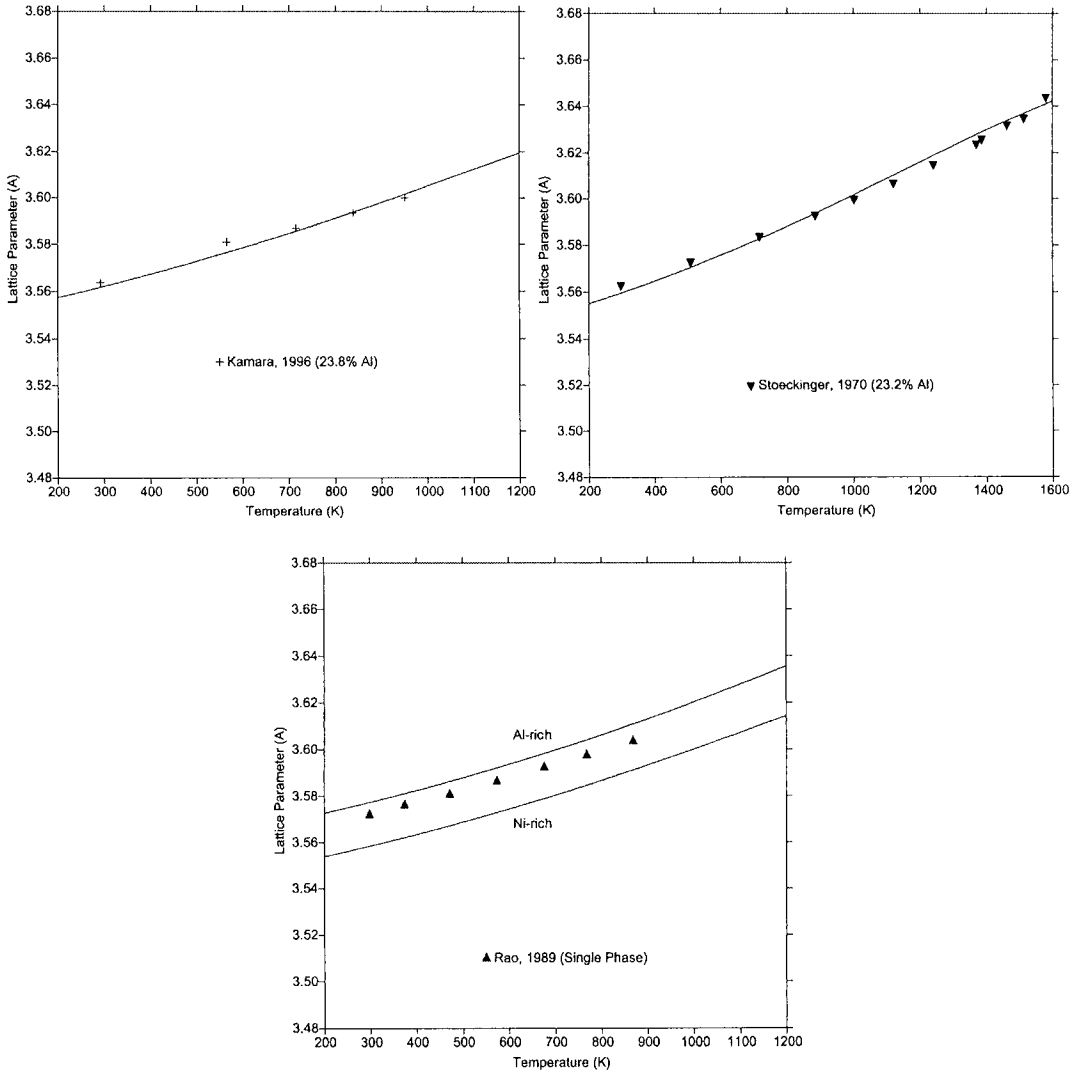

Fig. 10—Temperature dependence of the γ' lattice parameter (+, [32] ▼, [45] and ▲ [52]). The solid lines represent the results of the model calculation (S_N = 2.5×10^{-3} Å for Ref. 32 and $S_N = 2.7 \times 10^{-3}$ Å for Ref. 45).

respectively). On the other hand, Rao *et al.*[52] did not report the composition of their alloy. Their sample was prepared by arc melting and was homogenized at 1273 K and was found to be in the single-phase region by the metallographic method. Thus, the composition of their sample is probably between the Ni-rich part (23.0 at. pct Al) and the Al-rich part (27.3 at. pct Al) of the γ' single-phase region at 1273 K. The predicted values for these two compositions are plotted in Figure 10(c) as solid lines, and Rao's data lie between the two calculated curves and are closer to the Al-rich side of the γ' phase.

The relative thermal expansion of the γ' phase (25 at. pct Al) shown in Figure 11 is given by

$$\frac{\Delta a^{\gamma'}}{a^{\gamma'}_{293}} = \frac{a^{\gamma'} - a^{\gamma'}_{293}}{a^{\gamma'}_{293}} \qquad [26]$$

where $a^{\gamma'}_{293}$ is the lattice parameter of the γ' phase at 293 K. The calculated results (S_N = 0.06 pct) agree reasonably well with the experimental data.[23,36]

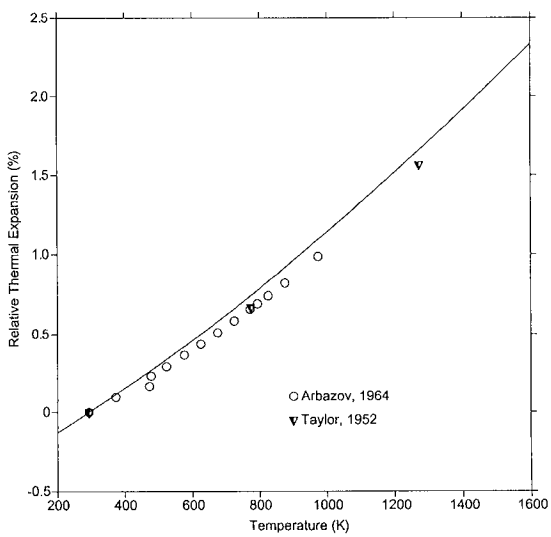

Fig. 11—The comparison of the experimental relative thermal expansion of the γ' phase (25 at. pct Al) (○ [23] and ▼ [36]) and the model calculation (solid line) (S_N = 0.06 pct).

C. *Mismatch between the γ and γ′ Phases*

The γ/γ' lattice mismatch (δ), defined as the relative difference of the lattice parameters of the matrix γ (a^{γ}) and the precipitate γ' ($a^{\gamma'}$),

$$\delta = \frac{a^{\gamma'} - a^{\gamma}}{0.5(a^{\gamma'} + a^{\gamma})} \qquad [27]$$

is considered to be an important microstructural quantity. Accurate lattice-mismatch data can be used to analyze the microstructural evolution and have been a focus of many investigations on commercial Ni-based alloys.[59,60]

The precipitation in a Ni-12.7 at. pct Al alloy aged at 973 K was studied by Phillips;[48] the mismatch data were calculated from the lattice parameters obtained by X-ray measurements on the quenched sample. Kamara *et al.*[32] aged a Ni-17.7 at. pct Al alloy at 973 K for 168 hours and measured the lattice parameters of the γ and γ' phases at different temperatures (293, 563, 713, 843, and 953 K) by high-temperature X-ray diffractometry. From those data, they calculated the corresponding mismatches.

Using the results from the present work, the lattice mismatch between the γ and γ' phases in the Ni-Al binary system were predicted and plotted in Figure 12. The solid curve shows the mismatch between the two equilibrium phases. On the other hand, as pointed out earlier, if the holding time is not long enough, the γ and γ' phases in the samples would maintain their compositions at the aging temperature (973 K), and their lattice parameters should, thus, be calculated using the corresponding equilibrium compositions at the aging temperature. The corresponding mismatches thus calculated are shown by the dashed line in Figure 12 for the aging temperature of 973 K.

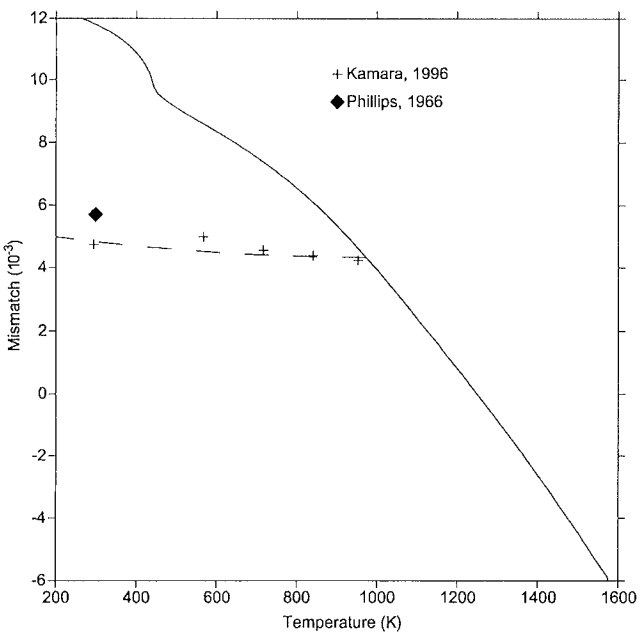

Fig. 12—The calculated mismatch between the γ and γ' phases (+[32] and ◆ [48]). The solid curve shows the mismatch under the equilibrium condition, and the dashed lines represent those under the frozen composition assumption ($S_N = 4.1 \times 10^{-4}$).

Since an accurate determination of the γ-γ' lattice mismatch in the laboratory is often difficult because it is very sensitive to the experimental conditions, such as sample preparation[61] and aging time,[62] the data reported by Phillips[48] and Kamara *et al.*[32] can be considered to be well represented by the present calculations ($S_N = 4.1 \times 10^{-4}$).

Furthermore, as shown in Figure 12, the lattice-mismatch value decreases with increasing temperature and crosses zero at around 1252 K. This phenomenon is also supported by several experimental investigations in commercial Ni-based superalloys.[5,32,63–65]

IV. CONCLUSIONS

A phenomenological model is developed to describe the lattice parameters of a substitutional solid solution. The lattice parameters of the pure elements are modeled under the assumption of a linear temperature dependence of thermal expansion, and those for solution phases are treated by an approach similar to that used in the Gibbs-energy modeling. This model has been applied to the Ni-Al system. Most available lattice-parameter data of the γ and γ' phases in the Ni-Al system can be reproduced, and the γ-γ' lattice mismatch can also be reasonably predicted by taking into account the slow diffusion during the measurement.

ACKNOWLEDGMENTS

The authors are grateful for the financial support from the NASA UEET program under Grant No. NCC3-920.

REFERENCES

1. M.L. Bhatia, A.K. Singh, and T.K. Nandy: *Intermetallics,* 1998, vol. 6, pp. 141-46.
2. L. Vegard: *Z. Phys.,* 1921, vol. 5, pp. 17-26.
3. H.W. King: *J. Mater. Sci.,* 1966, vol. 1, pp. 79-90.
4. B. Sundman and J. Agren: *J. Phys. Chem. Solids,* 1981, vol. 42, pp. 297-301.
5. M.V. Nathal, R.A. Mackay, and R.G. Garlick: *Mater. Sci. Eng.,* 1985, vol. 75, pp. 195-205.
6. D.F. Lahrman, R.D. Field, R. Darolia, and H.L. Fraser: *Acta Metall.,* 1988, vol. 36, pp. 1309-20.
7. F.R.N. Nabarro: *Metall. Mater. Trans. A,* 1996, vol. 27A, pp. 513-30.
8. H. Mughrabi and U. Tetzlaff: *Adv. Eng. Mater.,* 2000, vol. 2, pp. 319-26.
9. A.R. Ruffa: *J. Mater. Sci.,* 1980, vol. 15, pp. 2268-74.
10. F.L. Uffelmann: *Phil. Mag.,* 1930, vol. 10, pp. 633-59.
11. L. Catz: *Proc. Phys. Soc.,* 1955, vol. 68, p. 957.
12. P.D. Pathak and N.G. Vasavada: *J. Phys. C,* 1970, vol. 3, pp. L44-L48.
13. O. Redlich and A.T. Kister: *Ind. Eng. Chem.,* 1948, vol. 40, pp. 345-48.
14. J.O. Andersson, A.F. Guillermet, M. Hillert, B. Jansson, and B. Sundman: *Acta Metall.,* 1986, vol. 34, pp. 437-45.
15. I. Ansara, B. Sundman, and P. Willemin: *Acta Metall.,* 1988, vol. 36, pp. 977-82.
16. Y.S. Touloukian, R.K. Kirby, R.E. Taylor, and P.D. Desai: *Thermophysical Properties of Matter,* IFI-Plenum, New York, NY, 1975, vol. 12.
17. K. Wang and R.R. Reeber: *Phil. Mag. A,* 2000, vol. 80, pp. 1629-43.
18. J.F. Kenney and E.S. Keeping: *Mathematics of statistics,* Pt. 1, Princeton, New York, NY, 1962.
19. T.G. Kollie: *Phys. Rev. B,* 1977, vol. 16, pp. 4872-81.
20. G.D. Mukherjee, C. Bansal, and A. Chatterjee: *Int. J. Mod. Phys. B,* 1998, vol. 12, pp. 449-70.
21. M. Yousuf, P.C. Sahu, H.K. Jajoo, S. Rajagopalan, and K.G. Rajan: *J. Phys. F, Met. Phys.,* 1986, vol. 16, pp. 373-80.
22. Y. Tianji: *J. Phys. Soc. Jpn.,* 1971, vol. 31, pp. 1366-73.
23. M.P. Arbuzov and I.A. Zelenkov: *Phys. Met. Metallogr. (Russia),* 1964, vol. 18, pp. 149-50.

24. H.W. Altman, T. Rubin, and H.L. Johnston: Cryogenic Laboratory Report No. OSU-TR-264-27, Ohio State University, Columbus, OH, 1954, p. 10.
25. F.C. Nix and D. Macnair: *Phys. Rev.,* 1941, vol. 60, pp. 597-605.
26. A.S. Pavlovic, V.S. Babu, and M.S. Seehra: *J. Phys.-Condes. Matter,* 1996, vol. 8, pp. 3139-49.
27. V.V. Makeev and P.S. Popel: *High Temp.,* 1990, vol. 28, pp. 525-29.
28. J. Bandyopadhyay and K.P. Gupta: *Cryogenics,* 1977, vol. 17, pp. 345-47.
29. R. Kohlhaas, P. Dunner, and P.N. Schmitz: *Z. Angew. Phys.,* 1967, vol. 23, pp. 245-49.
30. T.A. Faisst: *J. Phys.-Condes. Matter,* 1989, vol. 1, pp. 5805-10.
31. J. Bottiger, N. Karpe, J.P. Krog, and A.V. Ruban: *J. Mater. Res.,* 1998, vol. 13, pp. 1717-23.
32. A.B. Kamara, A.J. Ardell, and C.N.J. Wagner: *Metall. Mater. Trans. A,* 1996, vol. 27A, pp. 2888-96.
33. Y.Y. Qiu: *J. Mater. Sci.,* 1996, vol. 31, pp. 4311-19.
34. G. Ayub, F.A. Khwaja, A.U. Haq, and Z. Ahmad: *Acta Metall. Mater.,* 1995, vol. 43, pp. 1457-65.
35. T. Tarfa, B. Sitaud, and O. Dimitrov: *Acta Metall. Mater.,* 1993, vol. 41, pp. 3191-202.
36. A. Taylor and R.W. Floyd: *J. Inst. Met.,* 1952-1953, vol. 81, pp. 25-32.
37. Y. Mishima, S. Ochiai, and T. Suzuki: *Acta Metall.,* 1985, vol. 33, pp. 1161-69.
38. P.V.M. Rao, K.S. Murthy, S.V. Suryanarayana, and S.V.N. Naidu: *J. Mater. Res.,* 1993, vol. 8, pp. 741-44.
39. C. Bertrand, J.P. Dallas, J. Rzepski, N. Sidhom, M.F. Trichet, and M. Cornet: *Mem. Etud. Sci. Rev. Met.,* 1989, vol. 86, pp. 334-46.
40. I. Baker, B. Huang, and E.M. Schulson: *Acta Metall.,* 1988, vol. 36, pp. 493-99.
41. Y.G. Kim, G.L.W. Yoon, and N.S. Stoloff: *J. Mater. Sci. Lett.,* 1985, vol. 4, pp. 1407-08.
42. S.C. Huang, A.I. Taub, and K.M. Chang: *Acta Metall.,* 1984, vol. 32, pp. 1703-07.
43. O. Noguchi, Y. Oya, and T. Suzuki: *Metall. Trans. A,* 1981, vol. 12A, pp. 1647-53.
44. K. Aoki and O. Izumi: *J. Jpn. Inst. Met.,* 1975, vol. 39, pp. 1282-89.
45. G.R. Stoeckinger and J.P. Neumann: *J. Appl. Crystallogr.,* 1970, vol. 1, pp. 32-38.
46. C.L. Corey and B. Lisowsky: *Trans. TMS-AIME,* 1967, vol. 239, pp. 239-43.
47. E. Hornbogen and M. Roth: *Z. Metallkd.,* 1967, vol. 58, pp. 842-55.
48. V.A. Phillips: *Acta Metall.,* 1966, vol. 14, pp. 1533-47.
49. M.P. Arbuzov and I.A. Zelenkov: *Fiz. Metall. Metalloved.,* 1963, vol. 15, pp. 725-28.
50. R.W. Guard and J.H. Westbrook: *Trans. TMS-AIME,* 1959, vol. 215, pp. 807-14.
51. A.J. Bradley and A. Taylor: *Proc. R. Soc.,* 1937, vol. A159, pp. 56-72.
52. P.V.M. Rao, S.V. Suryanarayana, K.S. Murthy, and S.V.N. Naidu: *J. Phys., Condens. Matter,* 1989, vol. 1, pp. 5357-61.
53. N. Dupin, I. Ansara, and B. Sundman: *CALPHAD,* 2001, vol. 25, pp. 279-98.
54. I. Ansara, N. Dupin, H.L. Lukas, and B. Sundman: *J. Alloy Compounds,* 1997, vol. 247, pp. 20-30.
55. J.O. Andersson, T. Helander, L.H. Hoglund, P.F. Shi, and B. Sundman: *CALPHAD,* 2002, vol. 26, pp. 273-312.
56. A. Engstrom and J. Agren: *Z. Metallkd.,* 1996, vol. 87, pp. 92-97.
57. H. Numakura, T. Ikeda, M. Koiwa, and A. Almazouzi: *Phil. Mag. A,* 1998, vol. 77, pp. 887-909.
58. H.A. Moreen, R. Taggart, and D.H. Polonis: *Metall. Trans.,* 1971, vol. 2, pp. 265-68.
59. H. Biermann, H. Mughrabi, and M. Strehler: *Metall. Mater. Trans. A,* 1996, vol. 27A, pp. 1003-14.
60. A. Royer, P. Bastie, and M. Veron: *Acta Mater.,* 1998, vol. 46, pp. 5357-68.
61. R.F. Decker and J.R. Mihalisin: *ASM. Trans. Q.,* 1969, vol. 62, pp. 481-89.
62. D.Q. Wang, S.S. Babu, E.A. Payzant, P.G. Radaelli, and A.C. Hannon: *Metall. Mater. Trans. A,* 2001, vol. 32A, pp. 1551-52.
63. S. Yoshitake, T. Yokokawa, K. Ohno, H. Harada, and M. Yamazaki: *Materials for Advanced Power Engineering 1994,* Part I, Liege, Belgium, Kluwer Academic Publishers Group, Dordrecht, Netherlands, 1994, pp. 875-82.
64. I.L. Svetlov, I.V. Oldakovskii, N.V. Petrushin, and I.A. Ignatova: *Russ. Metall.,* 1991, pp. 139-45.
65. G.N. Maniar and E.J. Bridge: *Metallography,* 1972, vol. 5, pp. 91-93.
66. F.R. Kroeger and C.A. Swenson: *J. Appl. Phys.,* 1977, vol. 48, pp. 853-64.
67. B. Guerard, H. Peisl, and R. Zitzmann: *Appl. Phys.,* 1974, vol. 3, pp. 37-43.
68. J.G. Collins and G.K. White: *J. Low Temp. Phys.,* 1973, vol. 10, pp. 69-77.
69. A.J.C. Wilson: *Proc. Phys. Soc.,* 1942, vol. 54, pp. 487-91.
70. K. Honda and Y. Okubo: *Sci. Rep. Tohoku Univ.,* 1924, vol. 13, pp. 101-07.
71. G. Langelaan and S. Saimoto: *Rev. Sci. Instrum.,* 1999, vol. 70, pp. 3413-17.
72. A.J. Cornish and J. Burke: *J. Sci. Instrum.,* 1965, vol. 42, pp. 212-18.
73. H.M. Otte, W.G. Montague, and D.O. Welch: *J. Appl. Phys.,* 1963, vol. 34, pp. 3149-50.
74. R.O. Simmons and R.W. Balluffi: *Phys. Rev.,* 1960, vol. 117, pp. 52-61.
75. R. Feder and A.S. Nowick: *Phys. Rev.,* 1958, vol. 109, pp. 1959-63.
76. F.A. Mauer, R.G. Munro, G.J. Piermarini, and S. Block: *J. Appl. Phys.,* 1985, vol. 58, pp. 3727-30.
77. I.M. Robertson and C.M. Wayman: *Metallography,* 1984, vol. 17, pp. 43-55.
78. R.S. Mints, G.F. Belyaeva, and Y.S. Malkov: *Russ. J. Inorg. Chem.,* 1962, vol. 7, pp. 1236-39.